Closed almost-periodic orbits in semiclassical quantization of generic polygons

Debabrata Biswas
Theoretical Physics Division, Bhabha Atomic Research Centre, Trombay, Mumbai 400 085, India

(Received 17 August 1999; revised manuscript received 12 January 2000)

Periodic orbits are the central ingredients of modern semiclassical theories and corrections to these are generally nonclassical in origin. We show here that, for the class of generic polygonal billiards, the corrections are predominantly classical in origin owing to the contributions from closed almost-periodic (CAP) orbit families. Furthermore, CAP orbit families outnumber periodic families but have comparable weights. They are hence indispensable for semiclassical quantization.

PACS number(s): 05.45.Mt, 05.45.Ac

There exists an approximate dual relationship between the spectrum of quantum energy eigenvalues and the classical length spectrum of periodic orbits and this forms the central theme of modern semiclassical theories. This duality was first discovered for the case of hyperbolic dynamics where all periodic orbits are isolated and unstable [1] and it was subsequently extended to the case of marginally stable systems where periodic orbits occur in families [2]. In particular, within the class of billiard systems (particles moving freely inside an enclosure and reflecting specularly from the walls), such a duality exists for polygons that are marginally stable and where periodic orbits with even bounces occur in bands [3].

In general, there are other (weaker) *nonclassical* contributions that make the relationship only approximate [4] and must be included at finite energy. For special cases, however (the tilted stadium billiard [12] and the truncated hyperbola billiard [13]), there is a source of classical correction as well. The aim of this paper is to show that, for an entire class of systems, corrections to the periodic orbit sum are predominantly *classical* in origin and are due to closed almost-periodic orbits. Also, because they are more numerous and have weights comparable to those of periodic orbit families, such orbits are indispensable at finite energies. First, however, we shall outline the key steps leading to the *semiclassical trace formula* where periodic orbits are the sole classical ingredients.

A convenient starting point is the relation [1]

$$\sum_n \frac{1}{E-E_n} = \int dq G(q,q;E) \tag{1}$$

$$\simeq \int dq G_{s.c.}(q,q;E) \tag{2}$$

where G and $G_{s.c.}$ refer, respectively, to the exact and semiclassical energy dependent propagator (Green's function) and $\{E_n\}$ are the energy eigenvalues. The approximate propagator $G_{s.c.}$ is obtained from a Fourier transform of the semiclassical time dependent propagator [1] and for a billiard

$$G_{s.c}(q,q';E) = -\imath \sum \frac{1}{\sqrt{8\pi\imath k l(q,q')}} e^{\imath k l(q,q') - \imath \mu\pi/2}, \tag{3}$$

where the sum runs over all orbits at energy $E=k^2$ between q and q' having length $l(q,q')$ and μ is the associated Maslov index. For convenience, we have chosen the mass $m=1/2$ and $\hbar=1$.

In the limit $k\rightarrow\infty$, the amplitude term in Eq. (3) varies slowly and can be regarded as a constant. The contribution of a particular orbit thus depends solely on the rapidity with which its action changes as q is varied. For periodic orbits, the action $S(q,q)$ does not vary along the orbit. Further, if it occurs in a band, the action does not vary in the transverse direction either, and the q integration merely picks up the area a_p of the primitive band. Thus

$$\begin{aligned}\rho(E) &= \sum_n \delta(E-E_n) \\ &= -\frac{1}{\pi}\lim_{\epsilon\rightarrow 0} \text{Im}\frac{1}{E+i\epsilon-E_n} \\ &\simeq \rho_{av}(E) + \sum_p \sum_{r=1}^{\infty} \frac{a_p}{\sqrt{8\pi^3 k r l_p}}\cos(krl_p - \pi/4) \\ &\quad - \sum_{p'} \sum_{r'=1}^{\infty} \frac{l_{p'}}{4\pi k}\cos(kr' l_{p'}),\end{aligned} \tag{4}$$

where ρ_{av} is the average density of states and the sums over p and p' run over primitive *families* and (marginally stable) *isolated orbits*, respectively, having length l_p.

For an isolated *unstable* periodic orbit on the other hand, the transverse direction leads to closed orbits with actions that vary depending on the stability of the periodic orbit, and its contribution to the trace depends on the eigenvalues of the Jacobian matrix arising from a linearization of the transverse flow. In contrast, closed nonperiodic orbits generally have negligible weight since their action varies rapidly with q. In the case of the tilted stadium [12], however, there exists a *family* of closed nonperiodic orbits for which the variation of action across the family (bouncing between the straight edges) is small and its contribution can be of the same order as the bouncing-ball periodic orbit family in the zero-tilt stadium. Due to its close association with orbit families in straight-edged billiards, it is surprising to note that diffraction [6–11] is still considered the most significant source of

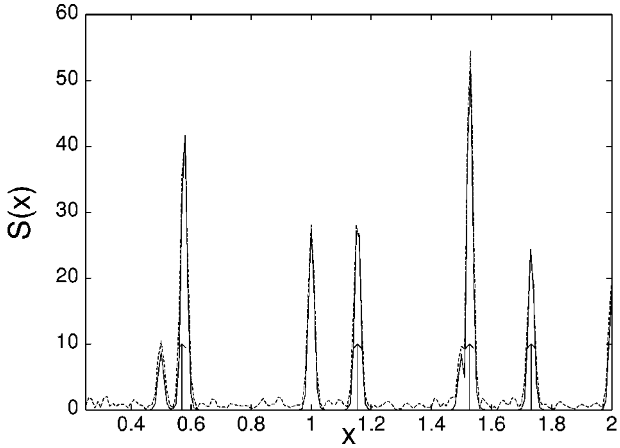

FIG. 1. Length spectrum $S(x)$ of the equilateral and $(1001\pi/3000,999\pi/3000)$ triangle (referred to as $T1$) The perimeter in both cases is 1. The arrows mark the positions of orbits that are periodic in the equilateral triangle but are almost periodic in $T1$. The full and dashed lines correspond to the equilateral and $T1$ triangles, respectively. In both cases, the first 1100 levels have been used to obtain $S(x)$.

correction in generic polygonal enclosures. While this is certainly true when the set of allowed momenta is small, generic polygons have additional classical contributions that are by far more important.

To underscore this point, consider an arbitrary polygon T_i obtained by perturbing another arbitrary polygon T. The slight change in the shape of the enclosure results in a slight change in the quantal eigenenergies so that the structure of the length spectrum $S(x)$ [the power spectrum of $\rho(k) = 2k\rho(E)$] is largely preserved and there are only minor variations in peak heights (see Fig. 1). However, the spectram of periodic orbit lengths in T and T_i are radically different as we shall shortly demonstrate. There is thus an apparent paradox which cannot be resolved by invoking diffraction since their contributions are $O(k^{-1})$ at best [15], compared to the $O(k^{-1/2})$ contributions of geometric periodic families.

The change in length spectrum of periodic orbits upon perturbation is best illustrated by comparing the equilateral and $T1$ triangles. As in the case of all rational polygons, the invariant surface of $T1$ is two dimensional and topologically equivalent to a sphere with g holes, where $g=1+(\mathcal{N}/2)\Sigma_i(m_i-1)/n_i$, $\{m_i\pi/n_i\}$ are the internal angles of the triangle, and $\mathcal{N}$ is the least common multiple of $\{n_i\}$. Thus for the $T1$ triangle, $g=1000$, while for the equilateral triangle, $g=1$. Note that the number of allowed momentum values is $2\mathcal{N}$ so that if $\mathcal{N}$ is large the probability that two segments of a trajectory have a small angle intersection is large. Thus, even though the boundary is only slightly perturbed, the structure of the invariant surface changes radically. It may thus be expected that the spectrum of periodic orbit lengths in the two systems will be very different as well. In the integrable case, these invariant trajectories live on the torus and are labeled by the winding numbers (M_1,M_2), which count the number of times the orbit goes around the two irreducible circuits. In the nonintegrable case, very little prior information is available [14], and we shall analyze the situation to demonstrate that the symbol sequences of periodic orbits in the equilateral triangle do not necessarily lead to periodic orbits in $T1$.

For the triangle enclosures, we shall use the symbols $\{1,2,3\}$ for the three sides [16]. A trajectory can then be labeled by a string of symbols $s_1s_2\cdots s_n$ where $s_i\in\{1,2,3\}$. Thus a sequence 1323 denotes a trajectory that reflects off sides 1, 3, 2, and 3 respectively. Let us denote by $R_i(i=1,3)$ the 2×2 reflection matrices of the three sides. These can be expressed in terms of the angle θ_i between the outward normal $(\hat{n}_i)$ to a side and the positive X axis,

$$R_i=\begin{pmatrix} -\cos(2\theta_i) & -\sin(2\theta_i) \\ -\sin(2\theta_i) & \cos(2\theta_i) \end{pmatrix}. \tag{5}$$

Thus, for the sequence 1323, the initial and final velocities are related by

$$\begin{pmatrix} v_x^f \\ v_y^f \end{pmatrix} = R_3\circ R_2\circ R_3\circ R_1 \begin{pmatrix} v_x^i \\ v_y^i \end{pmatrix} = R_{1323}\begin{pmatrix} v_x^i \\ v_y^i \end{pmatrix}, \tag{6}$$

where the superscripts $f(i)$ refer respectively to final (initial) velocities $\vec{v}$ whose components are v_x and v_y. It is easy to verify that when the number of reflections is odd

$$R_{s_1s_2\cdots s_n}^{(odd)}=\begin{pmatrix} -\cos(\varphi_o) & -\sin(\varphi_o) \\ -\sin(\varphi_o) & \cos(\varphi_o) \end{pmatrix}, \tag{7}$$

where $\varphi_o=2(\theta_1+\theta_3+\cdots+\theta_n)-2(\theta_2+\theta_4+\cdots+\theta_{n-1})$, while for an even number of reflections (n even),

$$R_{s_1s_2\cdots s_n}^{(even)}=\begin{pmatrix} \cos(\varphi_e) & \sin(\varphi_e) \\ -\sin(\varphi_e) & \cos(\varphi_e) \end{pmatrix}, \tag{8}$$

where $\varphi_e=2(\theta_1+\theta_3+\cdots+\theta_{n-1})-2(\theta_2+\theta_4+\cdots+\theta_n)$.

Obviously, the initial and final velocities can be equal if the resultant reflection matrix $R_{s_1s_2\cdots s_n}$ has a unit eigenvalue. For even n (the case of bands or families), the eigenvalues are $e^{\pm \imath\varphi_e}$ so that the condition for the existence of a unit eigenvalue is

$$\varphi_e=0 \mod(2\pi). \tag{9}$$

For odd n, on the other hand, the product of the eigenvalues $\lambda_1\lambda_2=1$. The eigenvector corresponding to a unit eigenvalue is $(\sin(\varphi_o/2),-\cos(\varphi_o/2))$ so that, if a real orbit exists with the sequence $s_1s_2\cdots s_n$, its initial and final velocities are equal.

In the event that a sequence repeats itself (denoted by $\overline{s_1s_2\cdots s_n}$) and there exists a unit eigenvalue of the resultant matrix $R_{s_1s_2\cdots s_n}$, stability considerations guarantee that a periodic orbit exists [19]. When n is odd, the orbit is isolated whereas when n is even the orbit exists in an equiaction family.

Not all sequences are allowed, however. Further, not all repeating sequences guarantee the existence of periodic orbits due to Eq. (9). For the $T1$ triangle, it is clear that the set of repeating sequences is the same as in the equilateral triangle for short orbits. Equation. (9), however, does not allow all of them to be periodic. For instance, the sequence 1323 results in a bouncing-ball family of periodic orbits in the

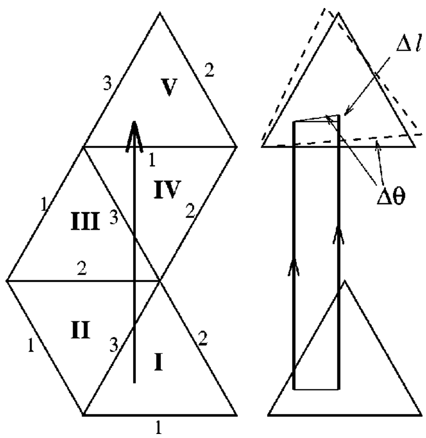

FIG. 2. The unfolded trajectory $\overline{3231}$ (marked by an arrow) is produced by successive reflections of triangle I to produce copies II, III, IV and V. For the equilateral case, copies I and V have the same orientation and the trajectory is periodic. For $T1$, the orientations differ slightly as shown schematically on the right. As a result the orbits are closed but nonperiodic.

equilateral triangle. In the $T1$ triangle, however, the eigenvalues for this sequence are $\exp(\pm\imath\pi/1500)$ so that there can be no periodic orbit with reflections from these sides. A sequence that is allowed, however, and leads to periodic orbit families in both triangles is 123123 (this is distinct from $\overline{123}$), since the periodicity condition [Eq. (9)] is automatically satisfied. In general, then, *for an arbitrary enclosure close to the equilateral triangle, an allowed sequence that repeats itself in the equilateral case can be a periodic family only when each symbol occurs as many times in even places as in odd places*. Thus, corresponding to the sequence 3231231231, there does not exist any periodic orbit in the $T1$ triangle while a periodic family exists in the equilateral case.

We have thus verified that the periodic orbits in the $T1$ and equilateral triangles are indeed different, even though short orbits follow the same sequences due to the proximity of the two triangles. Note that this observation holds in general for any arbitrary enclosure T. Upon perturbation, orbits follow the same sequence but the periodicity condition will not be satisfied for sequences that are periodic in T. According to Eq. (4) therefore, the peak positions and heights in the length spectrum should differ and we shall now show that the similarity in length spectrum observed in Fig. 1 is due to contributions from closed almost-periodic orbit families in $T1$.

Consider a symbol sequence that repeats itself and exists in both the equilateral and the $T1$ triangles. Further, assume that, corresponding to this sequence, there does not exist any periodic orbit in the $T1$ triangle while a periodic orbit family does exist in the equilateral case. Examples of these are the sequences $\overline{3231}$, $\overline{3231231231}$($l_p=1.5275$), and $\overline{2312312312312131}$($l_p=2.5166$). In every such case, one can construct ''unfolded'' trajectories (which are straight lines) by successive reflections of the triangle about the sides where the collision occurs. For instance (see Fig. 2), unfolded trajectories for the sequence 3231 can be created by first reflecting the triangle about side 3. The copy (II) so obtained is then reflected about side 2, the resultant copy (III) reflected about side 3, and finally (copy IV) about side 1. For the equilateral triangle, the final copy (V) has the same orientation as the initial copy (I) so that any line joining corresponding points in the initial and final copies is an ''unfolded periodic orbit.'' In the $T1$ triangle, however, the final copy differs marginally in orientation from the initial copy so that any line joining corresponding points in the two can only be a closed almost-periodic orbit. Obviously, at every point $\vec{q}$ there exists such a closed orbit with this sequence so long as the line joining the corresponding points (in I and V) lies entirely within the copies generated through reflections. Two such orbits separated by $q_\perp$ are shown in Fig. 2 (right). It is easy to see that the orbits differ in length by an amount $\Delta l = q_\perp \tan(\Delta\theta) \simeq q_\perp \Delta\theta$ if $\Delta\theta$ is small. Note that the above analysis holds for other almost-periodic closed orbits as well (such as the sequence 3231231231) and any arbitrary polygon T. In each of these cases $\Delta l \simeq q_\perp \Delta\theta = q_\perp \varphi_e$ so that the length varies slowly if the orbit nearly closes in momentum.

The correct trace formula for an arbitrary polygon T can be derived by noting that, for a closed almost-periodic family, $l(q_\perp) = l(0) + q_\perp \varphi_e$ where $l(0) = l_i$ is the length of the orbit in the center of the band and $q_\perp$ varies from $-w_i/2$ to $w_i/2$, where w_i is the transverse extent of the band. Assuming that k is sufficiently large, the amplitude $[1/l(q_\perp)]$ can be treated as a constant $(1/l_i)$ and the trace formula for finite k is then

$$\rho(E) \simeq \rho_{av}(E) + \sum_i \frac{a_i}{\sqrt{8\pi^3 k l_i}} \times \cos(kl_i - \pi/4) \frac{\sin(k\varphi_e^{(i)} w_i/2)}{k\varphi_e^{(i)} w_i/2} - \sum_{p'} \sum_{r'=1}^{\infty} \frac{l_{p'}}{4\pi k} \cos(kr' l_{p'}). \tag{10}$$

In Eq. (10), the sum over i runs over closed almost-periodic and periodic orbit families and l_i is the (average) length of such a family. Note that as $k \to \infty$ the contribution of almost-periodic orbits $(\varphi_e^{(i)} \neq 0)$ vanishes as $k^{-3/2}$, so that Eq. (10) reduces to Eq. (4). For de Broglie wavelength $\lambda \gg \pi w_i \varphi_e^{(i)}$, however, the ($i$th) closed almost-periodic orbit family contributes with a weight comparable to that of periodic families $[O(1/k^{1/2})]$ and hence assumes greater significance than diffraction [20]. Interestingly, such orbits clearly show up in eigenfunctions [21], and this has been referred to as ''scarring by ghosts of periodic orbits'' since such a periodic orbit exists only in a neighboring polygon. Thus a direct resolution of the paradox lies in closed almost-periodic orbits.

To emphasize the importance of the angle between the initial and final momentum (φ_e), we compare the power spectra of three different triangles, $T1$,$T2$, and $T3$ with the equilateral triangle in Fig. 3. For the sequence 3231, φ_e is maximum for $T3$ and minimum for $T1$ so that peak heights at 0.57 and its repetitions should be closest to those of the equilateral triangle for $T1$ and farthest for $T3$. This can indeed be verified from Fig. 3.

The contributions of closed almost-periodic (CAP) families diminish with energy in accordance with Eq. (10) and

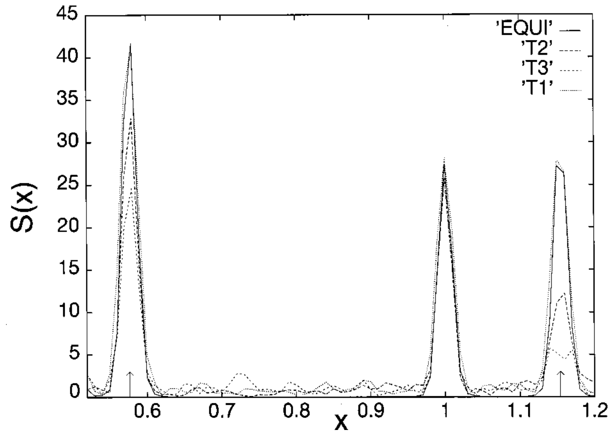

FIG. 3. A comparison of the length spectrum for four different triangles EQUI—equilateral, $T1$—$(1.001\pi/3, 0.999\pi/3, \pi/3)$, $T2$—$(1.01\pi/3, 0.99\pi/3, \pi/3)$, and $T3$—$(1.01513\pi/3, 0.98487\pi/3, \pi/3)$. The arrows are at 0.577 and 1.154, corresponding to the sequence 3231. In all cases, the first 1100 levels have been used to obtain $S(x)$. Note that $T1$ is practically indistinguishable from the equilateral curve while $T3$ is farthest from EQUI. The corresponding values of φ_e for the four cases are EQUI—0, $T1$—0.000667π, $T2$—0.006667π, and $T3$—0.010087π. In contrast, the peak at $x=1$ remains unchanged for all four triangles since it corresponds to a periodic orbit $(\overline{123123})$.

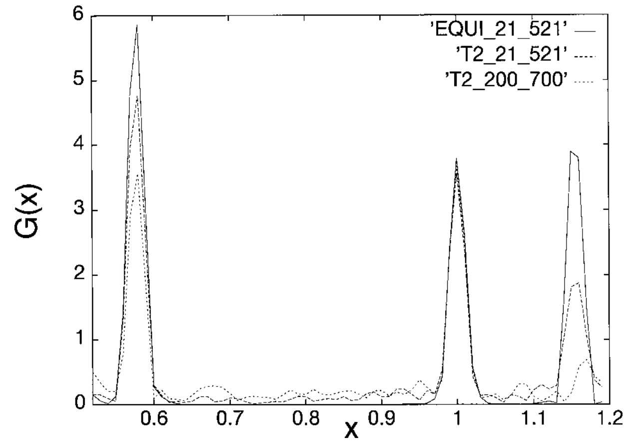

FIG. 4. A comparison of $G(x)$ for two energy ranges for the $T2$ triangle together with a typical plot for the equilateral triangle (marked EQUI_21_521 with $k_\alpha=21$ and $k_\beta=521$) when $k_\beta-k_\alpha=500$. Note the diminishing peak heights for the range $k\in(200,700)$.

can be observed in the length spectrum. In order to distinguish this from the contribution of periodic families, we shall consider the power spectrum G(x) of $\rho(k)/k^{1/2}$,

$$G(x)=\left|\sum_{k_\alpha\leqslant k_n\leqslant k_\beta}\frac{\cos(k_n x)}{k_n^{1/2}}+\imath\sum_{k_\alpha\leqslant k_n\leqslant k_\beta}\frac{\sin(k_n x)}{k_n^{1/2}}\right|, \tag{11}$$

such that for a fixed $k_\beta-k_\alpha$ the peak height of periodic families remains unaltered irrespective of k_β. Figure 4 show plots of $G(x)$ for the $T2$ triangle using two different k intervals, (21,521) and (200,700). In both cases, the peak height remains unaltered at $x=1.0$ corresponding to a periodic family. The peak at $x=0.57$, however, diminishes in height as the interval shifts to a higher energy. Also shown is a plot for the equilateral triangle which remains unchanged so long as $k_\beta-k_\alpha$ is fixed.

Precise checks (without using any window function) between the observed and expected peak height at $x=0.57$ show that the value expected from Eq. (10) is 11.3 while the observed height is 9.6. Undoubtedly, there are other sources of corrections, but the dominant contribution at this value of x is due to the closed almost-periodic family.

Finally, though the examples chosen are close to the $(\pi/3,\pi/3)$ triangle, we wish to reiterate that closed almost-periodic families contribute away from the neighborhood of integrable enclosures as well. To see this, consider an arbitrary triangle T. In its immediate neighborhood, there exists an infinity of triangles $\{T^{(i)}\}$, *each with a distinct periodic orbit spectrum* but having the same symbol sequence for short trajectories. Assume now that there exists a periodic orbit corresponding to the sequence S_k for the triangle $T^{(j)}$. Then, for all other triangles in its neighborhood, this sequence contributes an amount (nearly) equal to the periodic orbit contribution of $T^{(j)}$, provided $\pi w_i \varphi_e^{(i)} \ll \lambda$. Thus, corresponding to *every* periodic family in *each* of the triangles $\{T^{(i)}\}$, there exists an almost-periodic family in the triangle T whose contribution is comparable to that of periodic orbit families in these neighboring triangles.

To conclude, we have demonstrated that closed almost-periodic orbit families are more numerous than and have weights comparable to those of periodic families in polygonal billiards. They are thus indispensable for the semiclassical quantization of generic polygons.

[1] M. C. Gutzwiller, *Chaos in Classical and Quantum Mechanics* (Springer-Verlag, New York, 1990); in *Chaos and Quantum Physics*, Les Houches Session LII, 1989, M.-J. Giannoni, A. Voros, and J. Zinn-Justin (North-Holland, Amsterdam, 1991).

[2] M.V. Berry and M. Tabor, Proc. R. Soc. London, Ser. A **349**, 101 (1976).

[3] P.J. Richens and M.V. Berry Physica D **2**, 495 (1981).

[4] Contributions from diffractive orbits are the most relevant corrections in the present context [5–11].

[5] G. Vattay, A. Wirzba and P.E. Rosenqvist, Phys. Rev. Lett. **73**, 2304 (1994).

[6] Y. Shimizu and A. Shudo, Chaos, Solitons and Fractals **5**, 1337 (1995).

[7] N. Pavloff and C. Schmit Phys. Rev. Lett. **75**, 61 (1995).

[8] N.D. Whelan, Phys. Rev. Lett. **76**, 2605 (1996).

[9] H. Bruus and N.D. Whelan, Nonlinearity **9**, 1023 (1996).

[10] H. Primack, H. Schanz, U. Smilansky, and F. Ussishkin, Phys. Rev. Lett. **76**, 1615 (1996).

[11] M. Sieber, N. Pavloff, and C. Schmit, Phys. Rev. E **55**, 2279 (1997).

[12] H. Primack and U. Smilansky, J. Phys. A **27**, 4439 (1994).

[13] R. Aurich, T. Hesse, and F. Steiner, Phys. Rev. Lett. **74**, 4408 (1995).

[14] E. Gutkin, J. Stat. Phys. **83**, 7 (1996).
[15] E. Bogomolny, N. Pavloff, and C. Schmit, chao-dyn/9910037.
[16] A binary alphabet is enough to describe trajectories in triangles, though even this is cumbersome in practice since periodic orbit families proliferate only as a power law. For methods of finding periodic orbits, see [17,18].
[17] D. Biswas, Phys. Rev. E **54**, R1044 (1996).
[18] D. Biswas, Pramana, J. Phys. **48**, 487 (1997).
[19] D. Biswas, this issue, Phys. Rev. E **61**, 5073 (2000).
[20] Note that almost-periodic closed orbit families do not generally occur in systems where the number of directions accessible to a trajectory is small since the (average) angle of intersection is large. Thus diffraction is the principal source of correction in such cases.
[21] P. Bellomo and T. Uzer, Phys. Rev. E **50**, 1886 (1994).